J Mater Sci (2009) 44:2334–2342
DOI 10.1007/s10853-008-3197-6

FESTSCHRIFT IN HONOUR OF PROF T R ANANTHARAMAN ON THE OCCASION OF HIS 80TH BIRTHDAY

# Computational thermodynamics of Sc–Zr and Sc–Ti alloys using cluster variation method

**Shrikant Lele · B. Nageswara Sarma**

Received: 30 May 2008 / Accepted: 15 December 2008 / Published online: 22 January 2009


**Abstract** The cluster expansion method (for configurational enthalpy of mixing) and cluster variation method (for configurational entropy of mixing) (CE–CVM) together offer a systematic hierarchy of approximations for representation of phase diagram, thermochemical, thermophysical and structural data as opposed to the traditional CALPHAD methods which neglect the effects of local order and vibrational and electronic mixing contributions to the Gibbs function. The CE–CVM has not been very widely used for computation of phase equilibria since it is algebraically complex. A procedure has been developed for simultaneous nonlinear optimization of all the relevant data under the framework of CE–CVM. Vibrational and electronic mixing contributions have also been included using the CE method. The procedure has been successfully utilized for computing the solid-state regions of the phase diagrams of Sc–Zr and Sc–Ti. Debye temperatures and short-range order (sro) parameters have been calculated for these systems.

Professor Tanjore Ramachandra Anantharaman has directly or indirectly educated and influenced several generations of metallurgists and materials scientists in India. He has successfully established and nurtured the school of research in physical metallurgy and materials engineering at Banaras. It has been a rare privilege to be associated with him. The authors are happy to present this article in his honour on his 80th birthday.

S. Lele (✉) · B. N. Sarma
Centre of Advanced Study, Department of Metallurgical Engineering, Institute of Technology, Banaras Hindu University, Varanasi 221 005, India
e-mail: drslele@gmail.com

## Introduction

The cluster variation method (CVM) proposed by Kikuchi [1] as a theory of cooperative phenomena, provides a systematic hierarchy of approximations for obtaining configurational entropy of alloy systems by considering local order as accurately as desired in terms of increasingly larger atomic clusters. The potential of CVM came to be well recognized ever since van Baal [2] demonstrated the effect of tetrahedral multiatom interactions (in terms of a set of adjustable parameters in the configurational energy expression) on the topology of phase diagrams of a prototypical binary fcc ordering system. The phase diagram of the fcc-based Au–Cu system with an acceptable topology was, for the first time, obtained by Kikuchi and de Fontaine [3]. The CVM is also shown to subsume many of the earlier models in its class as lower levels of the general hierarchy of the method [4]. The tetrahedron–octahedron (T–O) approximation of CVM for close packed structures, which includes second neighbor interactions, successfully accounts for the stability of observed ground states as well as favorably compares with the Monte-Carlo calculations at finite temperatures [5]. On the other hand, an irregular tetrahedron (IT) includes these interactions in bcc structures and provides a good CVM approximation [6, 7]. Sanchez et al. [8] subsequently proved that any function depending on atomic configuration (such as configurational energy) could be rigorously expressed as a bilinear sum of the products of correlation functions and their respective cluster expansion coefficients (CECs), since the former form a set of complete and orthonormal basis functions at the chosen level of cluster approximation. This powerful property is utilized in the method of cluster expansions (CE), which, when combined with CVM makes it very versatile and eminently suitable for optimization purposes

[9] as well as in the use of first principles electron energy calculations for the determination of phase equilibria [10].

The CALPHAD techniques [11, 12] traditionally neglect the effects of short-range order (sro) and vibrational and electronic mixing contributions to the Gibbs function both of which are invariably present in alloy systems. The attempts to combine these with CVM are not entirely satisfactory, because all the effects of the so-called Unidentified Factors Overlooked [13] are treated in an empirical manner in terms of a Redlich–Kister polynomial. In the standard CALPHAD techniques, the model parameters are determined by optimization of experimental data using least-squares techniques as discussed by many authors [11, 12, 14, 15]. However, CVM has not been extensively used for computing optimized phase equilibria. The developments in and the applications of CVM are well documented by de Fontaine [10, 16], Finel [17], Saunders and Miodownik [11] and more recently by Inden [7].

In this investigation, CE–CVM has been used for obtaining optimized phase diagrams of binary alloy systems exhibiting disordered cph ($\alpha$) and bcc ($\beta$) phases, respectively, using the T–O and IT approximations. The configurational contribution to Gibbs functions of these phases is reviewed in section "Configurational thermodynamics of $\alpha$ and $\beta$ phases". The vibrational and electronic mixing contributions to Gibbs functions have been considered in the framework of CE–CVM in section "Vibrational and electronic contributions" by generalizing the expressions for pure components. A complete procedure for simultaneously optimizing the phase equilibria, thermochemical, thermophysical and structural data has been developed and presented in section "Determination of internal and phase equilibria" and "Simultaneous optimization". This procedure is illustrated in sections "The scandium–zirconium system" and "The scandium–titanium system" with reference to the solid-state regions of Sc–Zr and Sc–Ti phase diagrams, which exhibit only the above mentioned phases in the solid state. These diagrams respectively exhibit a congruent maximum and monotectoid + eutectoid reactions. The results are discussed in section "Discussion" and conclusions presented in section "Conclusions".

## Configurational thermodynamics of $\alpha$ and $\beta$ phases

In CE–CVM, one begins by choosing a basic or maximal cluster of sites in the structure which contains all sites up to a particular neighbor distance. The cluster sites are populated with the atomic species $A$ and $B$ to obtain atomic cluster configurations. An independent set of configuration variables for specifying the cluster configurations can be obtained through the use of occupation and site operators. The occupation operators are defined as under [7].

$$P_i^A(P_i^B) = 1 \quad \text{if } A(B) \text{ atom occupies site } i \text{ and} \\ = 0 \quad \text{otherwise} \tag{1}$$

For an orthogonal basis, the site operator is defined as follows:

$$\sigma_i = P_i^A - P_i^B \tag{2}$$

Using these definitions, we obtain

$$P_i^A = \tfrac{1}{2}(1 + \sigma_i) \text{ and } P_i^B = \tfrac{1}{2}(1 - \sigma_i) \tag{3}$$

A correlation function is defined as an average of the corresponding cluster function over all the sites in the structure. The cluster function in turn is equal to the product of appropriate site operators. Thus $\phi_1^\alpha = \langle\sigma_i\rangle$ and $\phi_2^\alpha = \langle\sigma_i\sigma_j\rangle$ correspond to the correlation functions for the phase $\alpha$ for the clusters formed, respectively, by a single site (point) and first neighbor pair sites if the sites $i$ and $j$ are first neighbor pairs. The set of correlation functions for all the subclusters and the basic cluster form an independent set of configuration variables. Similarly, a cluster variable is an average of the products of appropriate occupation operators. Thus, for example, $\rho_1^\alpha = \langle P_i^A\rangle = x_A^\alpha$ and $\rho_2^\alpha = \langle P_i^B\rangle = x_B^\alpha$ correspond to the fractions of $A$ and $B$ atoms while $\rho_3^\alpha = \langle P_i^A P_j^A\rangle$, $\rho_4^\alpha = \langle P_i^A P_j^B\rangle = \langle P_i^B P_j^A\rangle$ and $\rho_5^\alpha = \langle P_i^B P_j^B\rangle$ correspond to the fractions of first neighbor $AA$, $AB$, $BA$ and $BB$ pair configurations, respectively, on the cluster of first neighbor pair sites $i$ and $j$ for the phase $\alpha$. Clearly, these cluster variables are functions of the correlation functions and can be expressed as their linear functions by substituting from Eqs. 3. Thus $\rho_1^\alpha = \rho_1^\alpha(\phi_1^\alpha)$, $\rho_2^\alpha = \rho_2^\alpha(\phi_1^\alpha)$, $\rho_3^\alpha = \rho_3^\alpha(\phi_1^\alpha, \phi_2^\alpha)$, $\rho_4^\alpha = \rho_4^\alpha(\phi_1^\alpha, \phi_2^\alpha)$ and $\rho_5^\alpha = \rho_5^\alpha(\phi_1^\alpha, \phi_2^\alpha)$.

Analytical expressions for configurational mixing contributions to enthalpy, entropy and other thermodynamic functions of $\alpha$ phase are obtained earlier by McCormack et al. [18], using T–O approximation of CE–CVM. There are a total of 14 symmetry-wise distinct subclusters including the basic cluster (T–O), each of which corresponds to one cluster function and thus one correlation function $\phi_j^\alpha$ where $j$ is a serial number. The point correlation function is related to composition ($x_B^\alpha$) and thus, only 13 correlation functions remain independent for an alloy of fixed composition. These constitute the independent set of configurational variables for the phase $\alpha$. Because the configurational energy of mixing $H_c^\alpha$ is a function of configuration, it can be expanded using CE [7, 8] as in the following.

$$H_c^\alpha = \sum_{j=2}^{14} C_j^\alpha m_j^\alpha (\phi_j^\alpha)^{\text{mix}} \tag{4}$$

where $C_j^\alpha$ are configurational cluster expansion coefficients (CCECs), $m_j^\alpha$ are number of clusters of type $j$ per atomic site in the structure and $(\phi_j^\alpha)^{\text{mix}} = \phi_j^\alpha - (1 - x_B^\alpha)\phi_j^{\alpha,A} - x_B^\alpha\phi_j^{\alpha,B}$. Here, $\phi_j^{\alpha,A}$ and $\phi_j^{\alpha,B}$ represent the correlation

**Table 1** Cluster expansion coefficients (in J mol$^{-1}$) for Sc–Zr and Sc–Ti systems

| Cluster | Symbols | Sc–Zr | | Sc–Ti | |
|---|---|---|---|---|---|
| | | Configurational CEC | Vibrational CEC | Configurational CEC | Vibrational CEC |
| $\alpha$ phase | | | | | |
| In-plane pair | $C_2^\alpha$, $B_2^\alpha$ | −1297 | −0.03396 | −5777 | – |
| Out-of-plane pair | $C_3^\alpha$, $B_3^\alpha$ | −1297 | −0.03396 | −5777 | – |
| NNN pair | $C_4^\alpha$, $B_4^\alpha$ | – | – | – | – |
| Octahedral basal triangle | $C_5^\alpha$, $B_5^\alpha$ | – | – | 1015 | – |
| Tetrahedral basal triangle | $C_6^\alpha$, $B_6^\alpha$ | – | – | 1015 | – |
| Triangle inside octahedron | $C_7^\alpha$, $B_7^\alpha$ | – | – | – | – |
| Out-of-plane triangle | $C_8^\alpha$, $B_8^\alpha$ | – | – | 1015 | – |
| Tetrahedron | $C_9^\alpha$, $B_9^\alpha$ | – | – | 6863 | – |
| Rectangle inside octahedron | $C_{10}^\alpha$, $B_{10}^\alpha$ | – | – | – | – |
| Irregular tetrahedron inside octahedron (4-pt$^2$) | $C_{11}^\alpha$, $B_{11}^\alpha$ | – | – | – | – |
| Irregular tetrahedron inside octahedron (4-pt$^3$) | $C_{12}^\alpha$, $B_{12}^\alpha$ | – | – | – | – |
| Rectangular pyramid | $C_{13}^\alpha$, $B_{13}^\alpha$ | – | – | – | – |
| Octahedron | $C_{14}^\alpha$, $B_{14}^\alpha$ | – | – | – | – |
| $\beta$ phase | | | | | |
| I-neighbor pair | $C_2^\beta$, $B_2^\beta$ | −2724 | −0.009078 | −4170 | – |
| II-neighbor pair | $C_3^\beta$, $B_3^\beta$ | −1816 | −0.006052 | −2780 | – |
| Triangle | $C_4^\beta$, $B_4^\beta$ | – | – | 642 | – |
| Irregular tetrahedron | $C_5^\beta$, $B_5^\beta$ | – | – | −540 | – |

functions for pure components $A$ and $B$, respectively. The notations for clusters/subclusters for the cph structure and the corresponding CCECs are given in Table 1 [18].

The configurational entropy of mixing $S_c^\alpha$ can be expressed using CVM in terms of the cluster variables $\rho_k^\alpha(\phi_j^\alpha)$ and the (Kikuchi–Barker) overlap correction coefficients $\gamma_j^\alpha$ in the usual fashion as given below [7, 18].

$$S_c^\alpha = -R\sum_{j=1}^{14}\gamma_j^\alpha m_j^\alpha \sum_{k=1}^{43}\rho_k^\alpha(\phi_j^\alpha)\ln\rho_k^\alpha(\phi_j^\alpha) \quad (5)$$

The second sum runs over the number of all the distinct cluster variables for which the corresponding clusters have non-vanishing values of $\gamma_j^\alpha$ [18].

The procedures outlined above are adopted for the $\beta$ phase as well, under the IT approximation [6, 7, 19, 20]. A total of five symmetrywise distinct subclusters including the basic cluster (IT) are identified, each of which gives rise to one correlation function $\phi_j^\beta$ where $j$ is a serial number. Again, the point correlation function is related to composition ($x_B^\beta$) and thus, only four correlation functions remain independent for an alloy of fixed composition. These constitute the independent set of configurational variables for the $\beta$ phase. The notations for clusters/subclusters for the bcc structure and the corresponding CCECs are also given in Table 1. Further, there are 20 cluster variables $\rho_k^\beta(\phi_j^\beta)$ where $k$ is a serial number. The configurational energy and entropies of mixing for $\beta$ phase are expressed by equations similar to Eqs. 4 and 5.

## Vibrational and electronic contributions

### Pure components

Dinsdale [21] has published an evaluation of thermodynamic quantities for unary systems in terms of the following expansion

$$G_{ve} = a + bT + cT\ln(T) + \Sigma d_n T^n \quad (6)$$

in which, $a$, $b$, $c$ and $d$ are constants and $n$ represents a set of integers, typically taking the values of −1 and 2. On the other hand, the harmonic part of the vibrational contributions to thermodynamic functions can be represented by the following high temperature expansion [22]

$$G_v = RT\left[-1 + 3\ln\left(\frac{\theta_D(0)}{T}\right) + \frac{3}{40}\left(\frac{\theta_D(2)}{T}\right)^2\right] \quad (7)$$

where, $\theta_D(n)$ corresponds to cut-off frequencies $\omega_D(n)$ in a Debye model which reproduces correctly the $n$th moment of the vibrational frequency $\omega$ for a given phonon density of states. A comparison of terms in Eqs. 6 and 7 indicates

that $b$, $c$ and $d_{-1}$ are equal to $-R(1-3\ \ln\ \theta_D(0))$, $-3R$ and $-3R\theta_D^2(2)$ respectively. The term corresponding to $d_2$ in Eq. 6 is expected to represent the contributions due to anharmonic effects and electronic excitations.

The representation given by Dinsdale [21] for the unary system database considers only a linear dependence on $T$ (i.e., $A + B\ T$) for the differences in $c_p$ of different polymorphs of a metal, which is unrealistic and leads to problems. Further, a termwise comparison of the fitting equations of Dinsdale [21] with those in Eq. 7 in the above gives rise to unrealistic and thus unacceptable values of $\theta_D(n)$, such as negative temperatures in certain cases. In view of this, values for $\theta_D^{\alpha}(0)$ $(=\theta_D^{\alpha}(2))$ and $\theta_D^{\beta}(0)$ $(=\theta_D^{\beta}(2))$ have been taken from the assessment of Chen and Sundman [23] for the elements Hf, Ti and Zr. Then, the values of $d_2^{\alpha}$ and $d_2^{\beta}$ are estimated such that experimental values of $S^{\alpha}$ and $S^{\beta}$ are reproduced at the respective transformation temperatures in the case of Ti and Zr. For the case of Sc, the value of $\theta_D^{\beta}(0)$ $(=\theta_D^{\beta}(2))$ was obtained from $\theta_D^{\alpha}(0)$ $(=\theta_D^{\alpha}(2))$ given by Chen and Sundman [23] by using the same (average) ratio $\theta_D^{\alpha}(0)$: $\theta_D^{\beta}(0)$, as that for Hf, Ti and Zr, while the remaining procedure for the estimation of $d_2^{\alpha}$ and $d_2^{\beta}$ was retained as such.

## Alloys

Only the configuration-dependent terms in Eq. 6 survive while considering the mixing contributions for alloys. These are obtained from

$$G_{ve}^{mix} = b^{mix}T + \sum d_n^{mix}T^n \tag{8}$$

Because the mixing quantities in these equations are dependent on atomic configuration, we shall use the method of CE to represent them. Accordingly, the mixing contributions to $b$ and $d_n$ for each phase are represented using equations similar to Eq. 4 having the following form

$$b^{mix} = \sum_{j=2}^{M} B_j m_j (\phi_j)^{mix} \tag{9}$$

where $M$ is equal to 14 and 5, respectively, for the phases $\alpha$ and $\beta$. The parameters $B_j$ and $D_{-1,j}$ represent the small, albeit crucial, mixing contributions arising from the vibrational effects. If it is assumed that the nature of the configurational dependence of $(\theta_D(n))^{mix}$ for different values of $n$ (0 and 2) is formally the same, then, these contributions can be represented sufficiently accurately in terms of a single set of CECs along with appropriate scaling factors, which can be found in the following manner. The mixing contribution to $\ln\ \theta_D(0)$ (written as $\ln\ \theta_D$ in the following paragraph for notational convenience) can be written as

$$\begin{aligned}(\ln\theta_D)^{mix} &= \ln\theta_D - (1 - x_B)\ln\theta_D^A - x_B\ln\theta_D^B \\ &= \ln\theta_D - \overline{\ln\theta_D}\end{aligned}$$

Let $\ln\ \theta_D$ be denoted by $\zeta$ and accordingly, $\zeta = \bar{\zeta} + \zeta^{mix}$.

Then, $\theta_D = \exp(\bar{\zeta} + \zeta^{mix})$ and

$$\theta_D^2 = \left[\exp\left(1 + \frac{\zeta^{mix}}{\bar{\zeta}}\right)\right]^{2\bar{\zeta}} = \exp(2\ \bar{\zeta}) \cdot \left[\exp\left(\frac{\zeta^{mix}}{\bar{\zeta}}\right)\right]^{2\bar{\zeta}}$$

Note that the ratio $(\zeta^{mix}/\bar{\zeta})$ is expected to be a small fraction. Hence, by expanding its exponential function in powers of this ratio and neglecting higher order terms and also taking a binomial expansion up to the first term, $\theta_D^2$ can be approximated as,

$$\theta_D^2 = \exp(2\bar{\zeta})(1 + 2\zeta^{mix}) = \exp(2\bar{\zeta}) + 2\exp(2\bar{\zeta})\zeta^{mix}$$

Thus, mixing contributions to $\theta_D^2$ can be written as

$$\begin{aligned}(\theta_D^2)^{mix} &= \exp(2\bar{\zeta}) - (1 - x_B)(\theta_D^A)^2 - x_B(\theta_D^B)^2 \\ &\quad + 2\exp(2\bar{\zeta})\zeta^{mix}\end{aligned}$$

This can be re-expressed as

$$\begin{aligned}(\theta_D^2)^{mix} &= (\theta_D^A)^{2(1-x_B)}(\theta_D^B)^{2x_B} - (1 - x_B)(\theta_D^A)^2 \\ &\quad - x_B(\theta_D^B)^2 + 2(\theta_D^A)^{2(1-x_B)}(\theta_D^B)^{2x_B}(\ln\theta_D)^{mix}\end{aligned}$$

The terms $(\theta_D^A)^{2(1-x_B)}(\theta_D^B)^{2x_B} - (1 - x_B)(\theta_D^A)^2 - x_B(\theta_D^B)^2$ are clearly configuration independent. These terms along with their respective coefficients in the $G_v$ expression in Eq. 7 are very small compared to the leading term in the same. Neglecting these, the configuration-dependent mixing contributions are thus given by

$$(\theta_D^2)^{mix} = 2(\theta_D^A)^{2(1-x_B)}(\theta_D^B)^{2x_B}\ (\ln\theta_D)^{mix} \tag{10}$$

This equation is valid for $(\theta_D^2(0))^{mix}$, but we assume that it is also applicable to $(\theta_D^2(2))^{mix}$. As mentioned earlier, this assumption avoids the requirement of an additional set of parameters to express $d_{-1}^{mix}$ in the form of a CE as used for $b^{mix}$ in Eq. 9. This procedure also retains the bilinear nature of the expansion in all the terms. It is, however, worth mentioning that if $\theta_D$ is expanded as a bilinear sum [24], the configuration-independent mixing terms are as large as 25% of the total mixing terms while they are minimal when $\ln\ \theta_D$ is expanded as given above. Accordingly, the latter has been used in this investigation and configuration-independent mixing contributions to $(\theta_D^2(2))^{mix}$ terms have been neglected. Mixing contributions to $d_2$ can be included in the same manner as that for $b$ in Eq. 9. These are, however, still smaller and have been neglected in this investigation. It may be noted that setting $B_j = 0$ (in Eq. 9) and $D_{n,j} = 0$ implies neglect of the vibrational and electronic mixing contributions. This, in fact, corresponds to the familiar Kopp–Neumann rule [22] according to which the alloy specific heat is equal to the weighted average of those of the

components. This choice thus accounts for the so-called linear contributions which does not involve any additional parameters and forms the reference state of the present formulation. The above procedures have been utilized to obtain vibrational and electronic mixing contributions for both the phases, for which, the equations are formally similar. Thus, the total mixing contributions to the thermodynamic functions can be evaluated.

## Determination of internal and phase equilibria

The mixing contributions to the Gibbs function, say, $G^{\alpha}$ of $\alpha$ phase are obtained by adding the configurational, vibrational and electronic contributions from Eqs. 4, 5, 8, 9 and 10.

$$G^{\alpha} = \sum_{j} \left[ C_j^{\alpha} + RT \left\{ 3 + \frac{6}{40T^2} \left( \theta_{\mathrm{D}}^{\alpha,A} \right)^{2(1-x_B^{\alpha})} \left( \theta_{\mathrm{D}}^{\alpha,B} \right)^{2x_B^{\alpha}} \right\} \times B_j^{\alpha} - \frac{T^2}{2} D_{2,j}^{\alpha} \right] m_j^{\alpha} (\phi_j^{\alpha})^{\mathrm{mix}} - TS_c^{\alpha} \tag{11}$$

The Gibbs function is a hierarchical function of CECs ($C_j^{\alpha}$, $B_j^{\alpha}$ and $\mathrm{D}_{2,j}^{\alpha}$) of this phase, the macroscopic thermodynamic variables ($x_B^{\alpha}$ and $T$) as well as the microscopic variables $\phi_j^{\alpha}$. The CECs constitute the set of model parameters, which characterize the system under consideration. Therefore, the CECs have to be determined through a simultaneous optimization of all types of available data for the system. The details of this procedure are presented in section "Simultaneous optimization".

For a specific set of CECs, when the state of the system corresponds to two-phase equilibrium between, say, $\alpha$ and $\beta$ phases, the macroscopic variables of these phases (namely, any pair among the triplet of variables $x_B^{\alpha}$, $x_B^{\beta}$ and $T$ for a chosen value of the third one) are determined such that equality of chemical potentials of each of the two components in the two phases is ensured ($\mu_A^{\alpha} = \mu_A^{\beta}$ and $\mu_B^{\alpha} = \mu_B^{\beta}$). The chemical potentials can be found from the Gibbs function given in Eq. 11 by using standard thermodynamic expressions. The thermodynamic functions must be evaluated using the equilibrium values of microscopic variables $\phi_j^{\alpha}$ which should be determined by minimizing the Gibbs function $G^{\alpha}$ with respect to $\phi_j^{\alpha}$ for chosen values of $x_B^{\alpha}$ and $T$ as well as the CECs. Minimization of the Gibbs function $G^{\alpha}$ requires that the following conditions be satisfied:

$$\left( \frac{\partial G^{\alpha}}{\partial \phi_j^{\alpha}} \right)_{x_B^{\alpha},T} = 0 \qquad \text{for } j = 2 \text{ to } M \tag{12}$$

It is, however, worth recognizing that $\phi_j^{\alpha}$ vary with macroscopic variables, which, in turn, vary with the parameters. These arguments are useful for finding analytical derivatives of the thermodynamic functions as illustrated below.

A variation in $x_B^{\alpha}$ alters $G^{\alpha}$ directly because of the change in $x_B^{\alpha}$ itself and indirectly through a change in the microscopic variables ($\phi_j^{\alpha}$) of the system since their values are altered due to a change in the conditions of internal equilibrium at the changed composition. Accordingly, for fixed values of CECs at a constant temperature $T$, the differential $\mathrm{d}G^{\alpha}/\mathrm{d}x_B^{\alpha}$ can be written as

$$\frac{\mathrm{d}G^{\alpha}}{\mathrm{d}x_B^{\alpha}} = \left( \frac{\partial G^{\alpha}}{\partial x_B^{\alpha}} \right)_{\phi_j^{\alpha},T} + \sum_{j} \left( \frac{\partial G^{\alpha}}{\partial \phi_j^{\alpha}} \right)_{x_B^{\alpha},T} \left( \frac{\mathrm{d}\phi_j^{\alpha}}{\mathrm{d}x_B^{\alpha}} \right) = \left( \frac{\partial G^{\alpha}}{\partial x_B^{\alpha}} \right)_{\phi_j^{\alpha}} \tag{13}$$

since, for internal equilibrium of the corresponding phase, the terms corresponding to partial derivatives of $G^{\alpha}$ with respect to $\phi_j^{\alpha}$ should vanish owing to Eq. 12. Similar simplifying arguments have been used for obtaining various differentials required for computing phase equilibria as well as for performing simultaneous optimization of data to determine the CECs of the system.

Internal equilibrium of a given phase as well as coexistence of two- or three-phases can be obtained using the Newton–Raphson (NR) method. The corrections to the variables during the iteration are selected such that all the constraints on the variables (if there are any) are satisfied. Initial values of the correlation functions are required for the implementation of the NR method for internal equilibrium. The point or random approximation is used for this purpose. For computation of phase equilibria, the experimental values of the composition or temperature can be used as initial values.

From Eq. 11 for the Gibbs function and corresponding equations for the enthalpy and entropy, it follows that these thermodynamic variables depend on the entire set of configurational, vibrational and electronic CECs ($C_j^{\alpha}$, $B_j^{\alpha}$ and $\mathrm{D}_{2,j}^{\alpha}$). As the chemical potentials are in turn found from the Gibbs function, the phase diagram data also depend on the entire set of configurational, vibrational and electronic CECs. Conversely, the determination of the entire parameter set of CECs depends on all thermodynamic and phase diagram data. On the other hand, it follows from Eq. 9 that the Debye temperatures depend only on the vibrational CECs ($B_j^{\alpha}$). Conversely, the determination of only the vibrational CECs depends on thermophysical property data typified by Debye temperatures.

## Simultaneous optimization

The $\chi^2$-merit function required for simultaneous optimization of various types of data is defined as the sum (over

all data points $i = 1$ to $N$) of squares of the ratios of the errors $\epsilon_i$ and the respective standard deviations $\sigma_i$. Thus,

$$\chi^2 = \sum_{i=1}^{N} \left(\frac{\epsilon_i}{\sigma_i}\right)^2 \tag{14}$$

The CECs which are the model parameters have to be chosen to minimize the merit function. In general, $\epsilon_i$ corresponds to the differences between the observed quantities and those calculated using the model under the conditions of experimentation. Data corresponding to three different types of variables have been considered for simultaneous optimization in the present investigation. In the case of phase equilibria data, when a transformation temperature is measured for an alloy of fixed composition (as in the case of dynamic Differential Thermal Analysis (DTA) type of measurements), the error definition will be

$$\epsilon_i = T_{\text{obs}} - T_{\text{calc}} \tag{15}$$

On the other hand, when the composition of a particular phase, which is in equilibrium with a second phase is determined at a fixed temperature (as in the case of static optical microscopy type of measurements), the error definition will become

$$\epsilon_i = x_{B,\text{obs}} - x_{B,\text{calc}} \tag{16}$$

Note that the measured composition corresponding to each of the two-phase boundaries at a given temperature is treated as an independent observation for optimization. The calculated values of the composition or temperature can be found from the equality of chemical potentials as mentioned in section "Determination of internal and phase equilibria". The error definitions for thermodynamic measurements are typified by

$$\epsilon_i = H^{\alpha}_{\text{obs}} - H^{\alpha}_{\text{calc}} \tag{17}$$

where $H^{\alpha}$ is the enthalpy of mixing at known values of $x^{\alpha}_B$ and $T$ for the $\alpha$ phase. The calculated value of the enthalpy can be found from an equation corresponding to Eq. 11 for the Gibbs function. A similar error definition is used for $(\ln \theta^{\alpha}_{\text{D}}(0))^{\text{mix}}$, where $\theta^{\alpha}_{\text{D}}(0)$ is the Debye temperature at known values of $x^{\alpha}_B$ and $T$ for the $\alpha$ phase. The calculated values of $\theta^{\alpha}_{\text{D}}(0)$ can be found from the model parameters using equations such as Eq. 9 and the equivalences given in section "Vibrational and electronic contributions". Thermodynamic measurements were not available for the systems considered in this study.

An appropriate choice of the error equation between (15) and (16) for phase diagram data is vital for obtaining good fits to the data. This choice depends on the slope of the measured phase boundary [25]. Data corresponding to nearly vertical phase boundaries in the $T$–$x$ diagram should be treated as static type and the error definition in (16) should be used, irrespective of the actual method of measurement. Similarly, data corresponding to nearly horizontal phase boundaries should be treated as dynamic type and the error definition in (15) should be used for optimization.

The standard deviation is taken to be 10 K on temperature measurements and 0.01 on composition measurements since the actual standard deviations calculated from multiple runs of experiments are not available in literature. Smaller values of standard deviation are used for accurate and reliable data such as invariant temperatures (0.1 K) so as to reflect the higher accuracy and also to ensure correct reproduction of the same. Standard deviations for thermochemical property data such as enthalpy are usually available along with the data and are of the order of 200 J mol$^{-1}$. The standard deviations for thermophysical property data such as those related to Debye temperatures, namely $(\ln \theta_{\text{D}}(0))^{\text{mix}}$ are taken to correspond to the errors reported on the experimental measurements.

The $\chi^2$-merit function is minimized with respect to a chosen set of CECs to determine their values using the Levenberg–Marquardt algorithm [26]. This elegant algorithm makes it possible to continuously switch from the steepest descent method (which ensures decrement in $\chi^2$) when the system is far from the minimum in $\chi^2$, to the NR method to exploit the super linear (quadratic) convergence as the system comes closer to the minimum. This is achieved by making the Hessian matrix (consisting of second-order differentials of $\chi^2$ with respect to CECs) diagonally dominant initially for obtaining the steepest descent-like step. As the diagonal dominance for this matrix is reduced, one obtains the NR-like step.

Among those sets of CECs which correspond to a minimum in $\chi^2$, it is important to be able to identify the statistically significant set of parameters for a simultaneous optimization of data so as to adequately represent the system. This set is known as the maximal set and can be identified by utilizing the $F$-test [27, 28]. The sequence of inclusion of these parameters in optimization is determined based on the following considerations. The configurational effects are generally dominant compared to the other effects. The minimal set consists of the first neighbor pair interactions (with the CECs corresponding to the in-plane and out-of-plane first neighbors being equal, $C^{\alpha}_2 = C^{\alpha}_3$, that is the interactions are assumed to be isotropic) for the $\alpha$ phase. However, for the $\beta$ phase, the second neighbor pair CEC is chosen to be equal to two-thirds of the first neighbor pair CEC ($C^{\beta}_3 = 2/3C^{\beta}_2$). This choice is partially justified by the fact that the second neighbor distance in the bcc case is only 15% greater than the first neighbor distance. Further, this choice makes the average multiplicity of the pairs in the $\beta$ phase equal to that for first neighbor pairs in the $\alpha$ phase. Thus, the minimal set for each phase usually consists of one independent parameter. For systems

displaying a high degree of asymmetry, it may be necessary to include triangle CECs in the minimal set for optimization to account for the same and obtain the correct topology of the phase diagram. Again assuming isotropic interactions for the α phase, we get one additional parameter corresponding to triangle interactions ($C_5^{\alpha} = C_6^{\alpha} = C_8^{\alpha}$). Similarly, we have one additional parameter corresponding to triangle interactions ($C_4^{\beta}$) for the $\beta$ phase. The $F$-test is utilized for including the CECs corresponding to any other interactions. At any stage, the CEC leading to the maximum reduction in $\chi^2$ (corresponding to the largest $F$-value) among the competing parameters is included in preference to others. This procedure is repeated for successive inclusion of other parameters. The maximal set of optimized parameters thus obtained is used for calculating the values corresponding to each of the experimental observations. The optimized phase diagram is obtained by calculating the sets of macroscopic variables corresponding to phase equilibria at various temperatures.

## The scandium–zirconium system

Beaudry and Daane [29] have determined the Sc–Zr phase diagram, based essentially on which, Palenzona and Cirafici [30] have contributed the latest evaluation, which may be consulted for details and other references. Low-temperature specific heat data were utilized by Betterton and Scarbrough [31] to evaluate $\theta_D(-3)$. These data have also been utilized in this optimization.

As indicated in section "Simultaneous optimization", the choice of error equation between (15) and (16) should be made based on the slope of the phase boundary, irrespective of the actual method of experimental determination. The entire data of Beaudry and Daane were determined by DTA measurements. If the data are treated as such and the corresponding error equation given in (15) is used, the resulting phase boundaries do not fit properly to the data, irrespective of the number of parameters used for optimization.

The $\theta_D(-3)$ data have been converted to the high-temperature entropy Debye temperatures $\theta_D(0)$ using the scaling factor of 0.86 as given by Chen and Sundman [23] for cph metals. These have then been utilized to find the observed $(\ln \theta_D(0))^{mix}$ values. These data have also been used for simultaneous optimization with a standard deviation of 0.025, which approximately corresponds to the error limits as reported by Betterton and Scarbrough [31].

The complete dataset consists of 31 points including Debye temperatures. The minimal set of two parameters consisting of first neighbor pairs in each phase yields a value of 209 for $\chi^2$. When two pair vibrational parameters were included in the optimization along with their configurational counterparts, the value of $\chi^2$ became 40. This value of $\chi^2$ is the lowest among those obtained for all other combinations of parameters. The maximal set of parameters is given in Table 1. The optimized phase diagram computed using this set along with the observed data is presented in Fig. 1, which is in good agreement with the observed data. The calculated congruent extremum is compared with the experimental data below.

Calculated: 27.3 at.% Zr, 1410 °C
Experimental: 30.0 at.%Zr, 1415 °C

The calculated values of $(\ln \theta_D(0))^{mix}$ were converted to $\theta_D(-3)$ values and are compared with the observed data of Betterton and Scarbrough [31] in Table 2. The agreement between the two sets is nearly within the error limits except for points at the Zr-rich end.

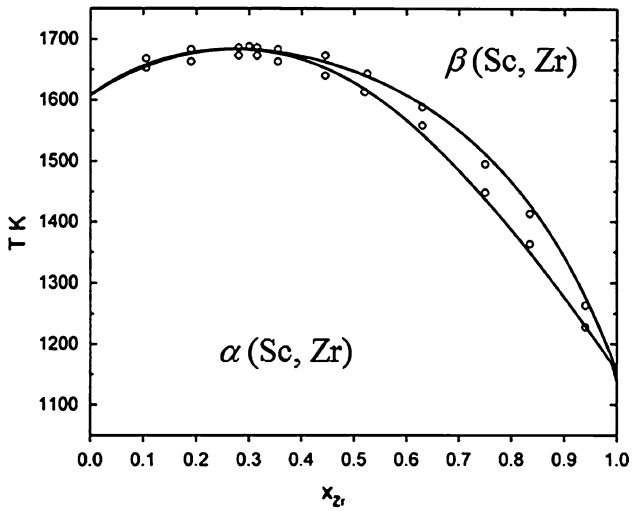


**Fig. 1** The scandium–zirconium phase diagram. The curves are computed from optimized parameters. The open circles represent thermal analysis data from Beaudry and Daane [32]

**Table 2** Observed and calculated Debye temperatures for Sc–Zr alloys

| $x_{Zr}$ | $\theta_D^{\alpha}(-3)$ (obs) K | $\theta_D^{\alpha}(-3)$ (calc) K |
|---|---|---|
| 0.00 | 306.0[a] | – |
| 0.11 | 360.0 ± 4.2 | 358.5 |
| 0.28 | 356.5 ± 10.2 | 352.0 |
| 0.49 | 344.1 ± 5.6 | 339.2 |
| 0.69 | 333.4 ± 2.3 | 323.3 |
| 0.80 | 333.1 ± 2.4 | 313.0 |
| 0.82 | 329.7 ± 3.4 | 311.0 |
| 0.89 | 310.6 ± 1.8 | 303.6 |
| 1.00 | 261.0[a] | – |

[a] Chen and Sundman [23]

### The scandium–titanium system

Murray [32] has assessed this system, essentially based on the work of Beaudry and Daane [33], who performed a comprehensive metallographic study as well as thermal analysis. The phase diagram in the solid-state region features a monotectoid reaction $\beta_1 = \alpha_1 + \beta_2$ at 1323 ± 10 K. At relatively low temperatures, the phase diagram exhibits a eutectoid reaction $\beta_2 = \alpha_1 + \alpha_2$ at 1148 ± 8 K. While the compositions of the solvus curves seem to be accurate up to ±1 at.%, the compositions of the phases in equilibrium at the monotectoid temperature are less accurate, because they are based on extrapolations of curves with low slopes to the invariant horizontal line.

Because the observed diagram exhibits considerable asymmetry, the minimal set chosen for this system consists of the triangle configurational CECs along with the pair CECs selected for the Sc–Zr system. The data set consists of 28 points and the value of $\chi^2$ for this minimal set is 116. Inclusion of two tetrahedral CECs leads to the largest decrement in $\chi^2$, to a value of 54. The maximal set of parameters is given in Table 1. The optimized phase diagram computed using the above set of parameters along with the selected data is presented in Fig. 2. It can be seen that the optimized phase diagram agrees well with the observed data. The invariant reactions are also reproduced very well in which, the deviations on compositions are usually about 1 at.% and those on temperatures are less than 1 K. The calculated and experimental compositions (refer to the figure given by Beaudry and Daane) and temperatures for the two invariant reactions are compared below.

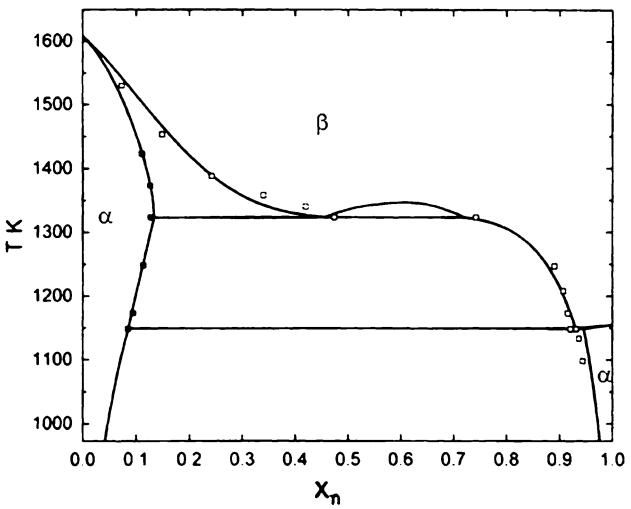


**Fig. 2** The scandium–titanium phase diagram. The curves are computed from optimized parameters. The open and filled squares represent thermal analysis and optical pyrometry data, respectively, from Beaudry and Daane [32]

Monotectoid reaction:

Calculated: 13.2, 47.5, 74.4 at.%Ti, 1,050 °C
Experimental: 12.8 ± 1, 47.4 ± 3, 74.2 ± 3 at.%Ti, 1,050 ± 10 °C

Eutectoid reaction:

Calculated: 8.6, 92.6, 93.1 at.%Ti, 875 °C
Experimental: 8.5 ± 1, 92.1 ± 1, 93.1 ± 1 at.%Ti, 875 ± 8 °C

## Discussion

CE–CVM procedures have been adopted for simultaneous optimization of phase equilibria and thermophysical Debye temperature data. Vibrational mixing contributions have been included in a configuration-dependent manner, for the first time. This formulation is consistent with those of its subsystems, which is a natural requirement as pointed out by Hillert [13]. This is not possible in traditional CALPHAD methods. Further, they can be extended for multicomponent systems in a straightforward manner. These procedures have been successfully utilized for obtaining optimized phase diagrams of Sc–Zr and Sc–Ti systems. In both the cases, the computed phase diagrams are in close conformity with the observed data. In the case of Sc–Ti system, the invariant reactions are reproduced very well, within 1 K and 1 at.%. The thermodynamic assessment due to Murray [32] reproduces the phase diagram equally well but cannot be used for the calculation of sro parameters as discussed below.

Because CVM treats local order accurately, sro parameters can be calculated using this approach, which is not possible in the standard CALPHAD approach. The Cowley–Warren [7] sro parameters (this is a variable in the present context) are given by

$$\sigma_{ij} = 1 - \frac{\langle P_i^A P_j^B \rangle}{x_A x_B} \tag{18}$$

The cluster variables in Eq. 18 can be computed from the corresponding pair correlation function at a chosen temperature and phase composition as discussed in section "Configurational thermodynamics of α and β phases". The pair correlation function can be determined by using the conditions for internal equilibrium as discussed in section "Determination of internal and phase equilibria". As an example, the first neighbor sro parameters for the $\beta$ phase have been calculated at three temperatures as a function of composition as shown in Fig. 3. It may be noted that at a temperature of 1000 K, the $\beta$ phase is either metastable or unstable for all compositions. The alloys are

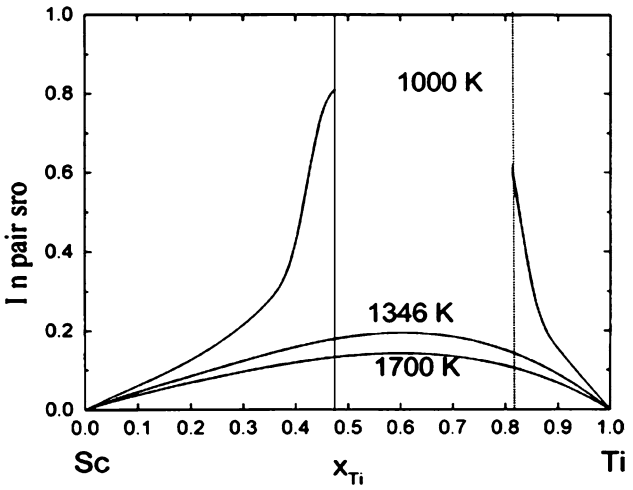


**Fig. 3** The Cowley–Warren first neighbor sro parameter for the $\beta$ phase as a function of composition at different temperatures calculated from the optimized parameters. The vertical lines represent spinodal compositions at 1000 K within which the $\beta$ phase is unstable

unstable within the range of spinodal compositions indicated by vertical lines in the figure and sro parameters cannot be calculated within this range. Such predictions of a structural parameter like the sro parameter for the stable/metastable regions of any phase are not possible in the standard CALPHAD framework. In addition, values of sro parameters can also be included in the optimization if such measurements are available.

## Conclusions

We have shown that binary systems exhibiting disordered phases can be optimized using data of different types such as phase diagram data, thermochemical data, thermophysical data (for example, Debye temperatures) and structural data (sro parameters) in the CE–CVM framework. Conversely, predictions can be made for each of these properties after optimization. This broad range of coverage is not possible using conventional CALPHAD methods. Vibrational and electronic mixing contributions have also been included using the CE method. These procedures have been successfully illustrated for the Sc–Zr and Sc–Ti systems. All the phase boundaries, invariant points, invariant reactions as well as thermophysical properties are reproduced very well. In addition, the model has enabled the calculation of a structural variable, namely, the sro parameter.

## References

1. Kikuchi R (1951) Phys Rev 81:988
2. van Baal CM (1973) Physica 64:571
3. Kikuchi R, de Fontaine D (1978) In: Applications of phase diagrams in metallurgy and ceramics. NBS Publication SP-496, p 967
4. Kikuchi R, Sato H (1974) Acta Metall 22:1099
5. Mohri T, Sanchez JM, de Fontaine D (1985) Acta Metall 33:1171
6. Ackermann H, Inden G, Kikuchi R (1989) Acta Metall 37:1
7. Inden G (2001) In: Kostorz G (ed) Phase transformations in materials. Wiley-VCH, Weinheim, p 519
8. Sanchez JM, Ducastelle F, Gratias D (1984) Physica 128A:334
9. Sarma BN (2000) Computation of optimized binary phase diagrams exhibiting CPH and BCC phases using cluster variation method. Ph.D. thesis, Banaras Hindu University, Varanasi
10. de Fontaine D (1994) Solid State Phys 47:33
11. Saunders N, Miodownik AP (1998) CALPHAD: a comprehensive guide. Pergamon, Oxford
12. Lukas HL, Fries SG, Sundman, B (2007) Computational thermodynamics—the calphad method. Cambridge
13. Hillert M (1997) Calphad 21:143
14. Lukas HL, Henig ETh, Zimmermann B (1977) Calphad 1:25
15. Bale CW, Pelton AD (1983) Metall Trans 14B:77
16. de Fontaine D (1979) Solid State Phys 34:73
17. Finel A (1994) In: Turchi PEA, Gonis A (eds) Statics and dynamics of alloy phase transformations, NATO ASI Series, Series B, Physics, vol 319. Plenum Press, New York, p 495
18. McCormack R, Asta M, de Fontaine D, Garbulsky G, Ceder G (1993) Phys Rev B 48:6767
19. Kikuchi R, van Baal CM (1974) Scr Metall 8:425
20. Kikuchi R (1987) Physica 142A:321
21. Dinsdale AT (1991) Calphad 15:317
22. Grimvall G (1986) Thermophysical properties of materials. North-Holland, Amsterdam
23. Chen Q, Sundman B (2001) Acta Metall 49:947
24. Asta M, McCormack R, de Fontaine D (1993) Phys Rev B 48:748
25. Lukas HL, Fries SG (1992) J Phase Equilib 13:532
26. Press WH, Teukolsky SA, Vetterling WT, Flannery BP (1993) Numerical recipes in C: The art of scientific computing. Cambridge University Press, Cambridge
27. Federer WT (1963) Experimental design. Oxford & IBH, New Delhi
28. Daniel C, Wood FS (1971) Fitting Equations to Data. Wiley-Interscience, New York
29. Beaudry BJ, Daane AH (1963) Trans TMS-AIME 227:865
30. Palenzona A, Cirafici S (1991) J Phase Equilib 12:53
31. Betterton JO Jr, Scarbrough JO (1968) Phys Rev 168:715
32. Murray JL (1987) Phase diagrams of binary titanium alloys. ASM International, Ohio, p 284
33. Beaudry BJ, Daane AH (1962) Trans TMS-AIME 224:770